

CHEMICAL SURFACE REACTIONS OF CO ON THE ATOMIC SCALE:
INVESTIGATIONS BY FIELD ION MICROSCOPY AND MASS SPECTROMETRY

J.H. Block and N. Kruse

Fritz-Haber-Institut der Max-Planck-Gesellschaft
Faradayweg 4-6, D-1000 Berlin 33

Received March 3, 1987

INTRODUCTION

Many modern problems in heterogeneous catalysis require highly sensitive microanalytical tools for surface analysis. One of the most sensitive methods to analyse a catalyst would be given if individual atoms or molecules at the catalyst surface could be identified. One would like to have a microscope with sufficient magnification to image a crystallographic plane on the atomic scale and to locate catalytically active sites in real space. The expert then wants to know the chemical composition at these sites and to learn where and how transient molecular species of a catalytic surface reaction are formed.

To the surprise of many scientists an instrument which can fulfill many of these demands exists since E.W. Müller developed the atom-probe [1]. This technique has been used in many different areas of surface and material science [2, 3]. In the present contribution applications of field ion microscopy and mass spectrometry to one problem of heterogeneous catalysis is reported. It has been shown in a large number of investigations that catalyst particles undergo changes in their crystallographic structure and morphology under catalytic reaction conditions at rather low temperatures. This phenomenon is investigated for the interaction of CO with Ni- and Ru-surfaces.

EXPERIMENTAL

Pulsed Field Desorption Mass Spectrometry (PFDMS) was applied in order to analyse on the atomic scale surface composition, binding states and mean

lifetimes of adsorbed intermediates during a catalytic reaction.

The apparatus, as described in detail in [4], consists of a field ion source, a channel plate image intensifier and a time-of-flight mass spectrometer. In this field ion time-of-flight device negative HV-pulses are applied to a counter-electrode, creating field pulses at the emitter surface with pulse heights $F_D \leq 50$ V/nm, pulse lengths ≥ 100 ns, and repetition rates of ≤ 100 kHz. Between the pulses, during the reaction time, t_R , (fig. 1) no field is applied for measurements of kinetic parameters. By changing the base field strength to sufficiently high values, however, still below the desorption of surface species, the field dependence of chemical reactions can be studied.

By the action of the very strong electric field pulse, adsorbed molecules and even surface lattice atoms are field desorbed (or field evaporated) in the form of ions. The mass/charge ratio of these ions is determined by a time-of-flight measurement. A probe hole technique selects a small surface area, containing a minimum of a few surface sites or up to several hundred surface atoms. Thus, we have a method to analyse a surface in real space with a lateral resolution on the scale of a few atomic sites.

The chemical analysis of surface-bound reactants, reaction interme-

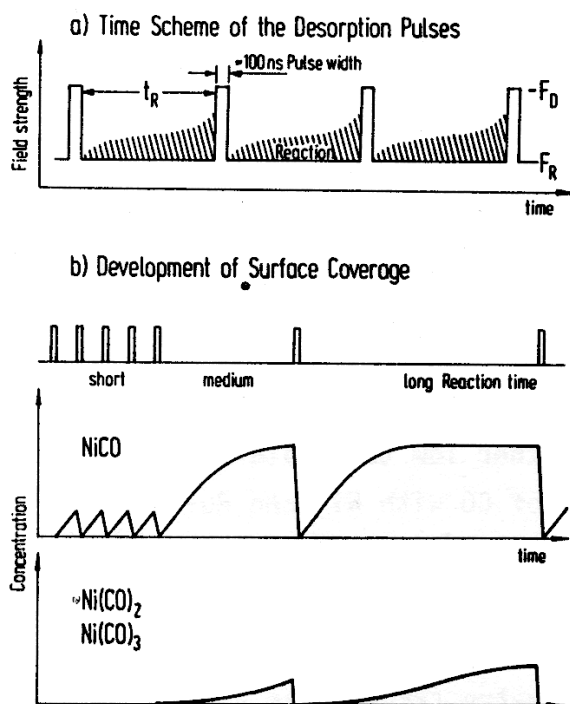


Fig. 1 Schematic diagram of field pulses with various repetition rates analysing the formation of physisorbed or chemisorbed particles as well as intermediates and products of a catalytic reaction.

diates or products on a catalyst, which has been given the shape of a field emitter tip, is one of the important features of this pulsed field desorption technique. The method is, however, not a straight-forward one. Several disturbing phenomena have to be considered in order to prevent misinterpretation of experimental data. The transformation of uncharged surface species into gaseous ions during field desorption is a complicated reaction phenomenon. Only after a detailed calibration, conclusions on the quality and quantity of neutral surface compounds can be drawn from the appearance of ionic species.

The experimental conditions have to be chosen such that the surface coverage of a species develops as shown in fig. 1. The impinging molecules accumulate during the reaction time (time interval t_R) between the pulses, and the next pulse desorbs the adlayer completely and analyses its composition quantitatively. Reactions occur within the adlayer, and the longer t_R , the more products are formed. Thus, the ion intensities depend on t_R , and they represent the development of the concentration, $c(t)$, with the starting condition of zero coverage. From the slope dc/dt at short times, the rate of the forward reaction can be deduced, and the value of t_R at which c levels off characterizes either a consecutive reaction or the back reaction. It even may happen, and was observed [5, 6] that the concentrations of intermediates can decrease again, so that there is a maximum at a certain t_R . The accessible time scale ranges from about 10 μ s to some minutes.

RESULTS AND DISCUSSIONS

The Interaction of CO with Ni-Surfaces

The topochemistry of this reaction was elucidated by field ion microscopic studies [7]. The reaction towards nickel tetracarbonyl is a surface site specific reaction, $\text{Ni} + 4 \text{CO} \rightarrow \text{Ni}(\text{CO})_4$, involving intermediate formation of adsorbed $\text{Ni}(\text{CO})_x$ species ($x < 4$). Preferential reactivity is found at the (111)-planes, where Ni atoms are removed from lattice sites along $\langle 001 \rangle$ rows. This follows from the crystallographic alterations during the formation of subcarbonyls [7] in fig. 2.

Fig. 2(a) shows an ion micrograph of the clean nickel crystal field evaporated in neon at 80 K. The middle part shows the relatively broadly

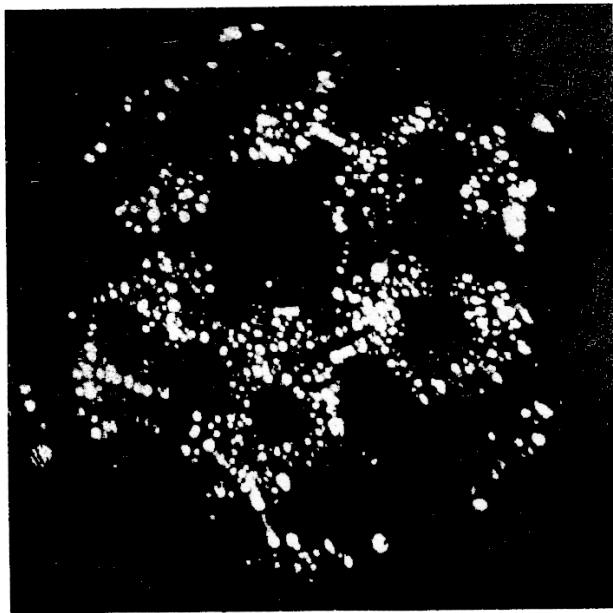
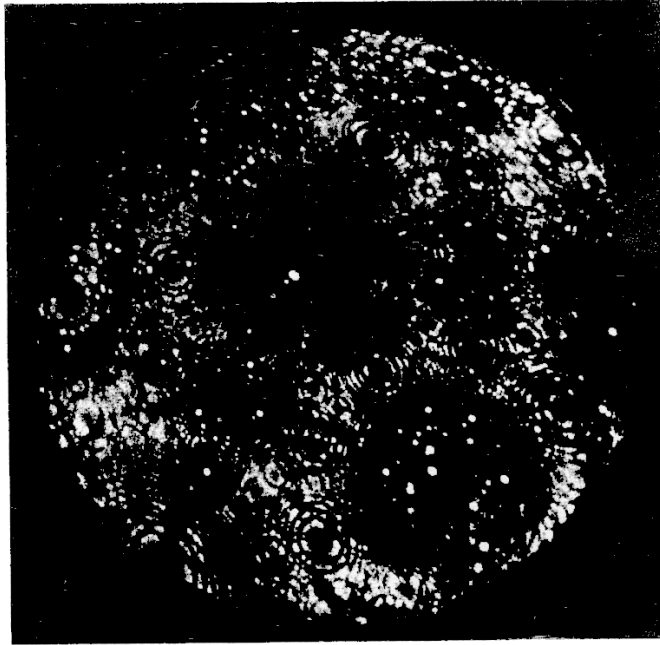


Fig. 2 (a) Field ion image of clean, nearly hemispherical nickel single crystal at 80 K, $F = 30.8 \text{ V/nm}$, image gas: neon. Radius of crystal calculated from central (111) area: $\sim 650 \text{ \AA}$, orientation about [311]. (b) The same nickel single crystal at 80 K, image gas neon, after reaction in CO, $p = 1.3 \text{ mbar}$ at 373 K.

extended system of (111)-layers. The step height of one layer is equal to the lattice step height. Slightly to the right in the lower part are the layers of the (100)-plane. The transient areas between the central (111) and the peripheral (111) and (100) planes are subdivided neatly up to very high index planes.

The surface structure of Fig. 2(b) was obtained after the crystal was under field-free reaction with CO at 1.3 mbar pressure at 373 K. In compari-

son to the initial state of the nickel crystal, there were conspicuous alterations of the crystal shape after reaction with CO:

1. Areas of $\{111\}$ planes were increased.
2. At half angles between the central $\{111\}$ and the peripheral $\{111\}$ planes there were $\{110\}$ planes flanked by $\{210\}$, and $\{100\}$ flanked by $\{511\}$, respectively. The small top layer of the $\{100\}$ planes showed within a cross a quadratic form in $\langle 110 \rangle$ orientation.
3. The number of rings around the $\{111\}$ poles was reduced compared with the initial state.

This alteration of crystal habitus can be explained by applying arguments of the theory of crystal growth. As discussed in detail in [7] this change in morphology has his reason in the high reaction rate of Ni-kink atoms of $\{111\}$ planes along $\langle 001 \rangle$ rows.

The mechanism of the intermediate carbonyl formation was studied by PFDMS [8]. In fig. 3 the time-dependence of the intermediates $\text{Ni}(\text{CO})$, $\text{Ni}(\text{CO})_2$ and $\text{Ni}(\text{CO})_3$ demonstrates a rather long delay time for the dicarbonyl.

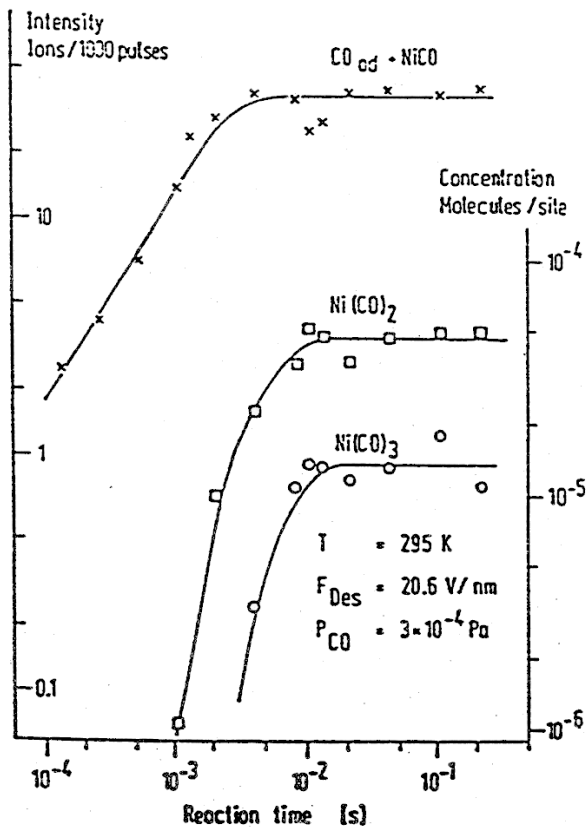


Fig. 3 Surface concentration of nickel subcarbonyls as function of reaction time t_R , monitored at an area of about 150 surface sites (impingement rate $\sim 450 \text{ CO/s}$).

From these results the conclusion can be drawn, that at least two CO-molecules have to be attached to a Ni kink site atom in order to remove it from the anchored lattice position. The mobile $\text{Ni}(\text{CO})_2$ surface species reacts to $\text{Ni}(\text{CO})_3$ and finally to $\text{Ni}(\text{CO})_4$ which is volatile and cannot be detected by our surface analytical tool.

The Reaction of CO with Ru-Surfaces

The crystallographic preferences of the carbonyl formation have not yet been studied by FIM. However, the stepped vicinity of the (0001)-pole proved to be a reactive area and was investigated by PFDMS. Various ionic species are detected. CO^+ , Ru^+ , Ru^{2+} as well as singly and doubly charged subcarbonyl species $\text{Ru}(\text{CO})_x^{n+}$ ($x=1\dots 4$, $n=1,2$) were observed besides some dissociation products and oxides [9, 10]. At the temperature of investigation, $T=328$ K, the intensities of the subcarbonyls depend on the desorption field strength, the reaction field strength and the reaction time.

The dependence on the desorption field strength, F_p , is shown in fig. 4. The surface binding and ionization energies differ for the various species because of their different onset values of the field strength. At low field strengths, F_p , only the CO^+ ion intensity is high. Here, adsorbed carbon monoxide is desorbed from a weakly bound physisorbed state. Its intensity fluctuations with increasing field strengths may be combined with diffusion and reaction phenomena towards carbonyls. The carbonyls $\text{Ru}(\text{CO})_3^{2+}$ and $\text{Ru}(\text{CO})_4^{2+}$ appear next to CO, however, at lower fields than $\text{Ru}(\text{CO})_2^{2+}$ and $\text{Ru}(\text{CO})^{2+}$. While the $\text{Ru}(\text{CO})_x$ -species ($x \geq 2$) are weakly chemisorbed intermediates of a consecutive surface reaction (see below), $\text{Ru}(\text{CO})^{2+}$ represents strongly bound CO.

The maximum intensities of $\text{Ru}(\text{CO})_x^{2+}$ ($x \geq 2$) indicate that respective neutrals are mobile. They can move from outside into the monitored area. However, at very high desorption fields the diffusion influence is suppressed and mobile surface species cannot reach the monitored area within the reaction time of 1 ms.

In contrast to nickel, the ruthenium subcarbonyl formation is strongly dependent on the reaction field, F_R . In fig. 5, F_R has been varied by keeping the desorption field constant at $F_D=29$ V/nm. For small F_R values considerable ion intensities of $\text{Ru}(\text{CO})_x^{2+}$ ($x=2-4$) are found, the RuCO^{2+} , how-

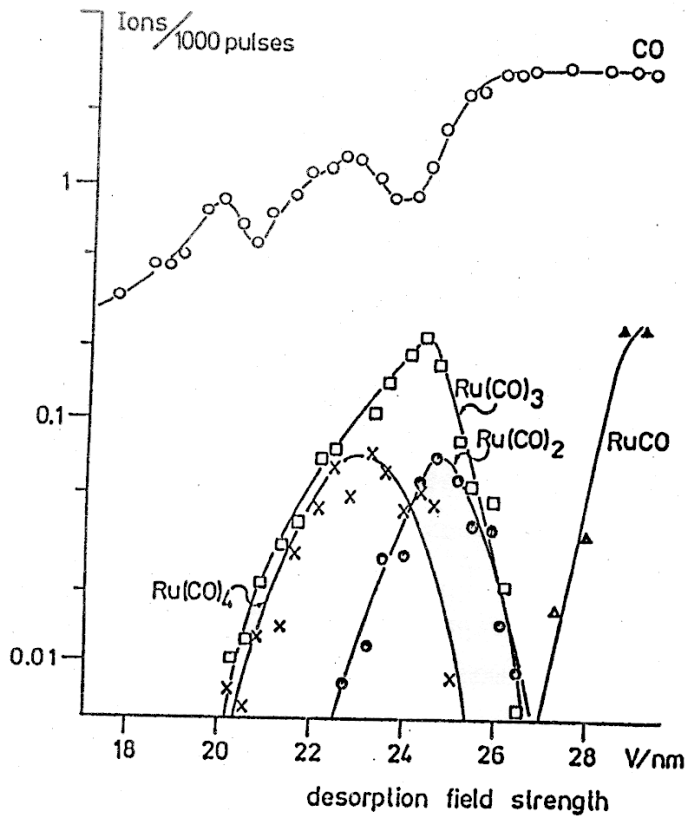


Fig. 4 Experimental intensities as function of the desorption field strength (pulses only, no steady field). Experimental parameters: $t_R=1$ ms, $T=328$ K, $p_{CO}=1.3 \cdot 10^{-4}$ Pa.

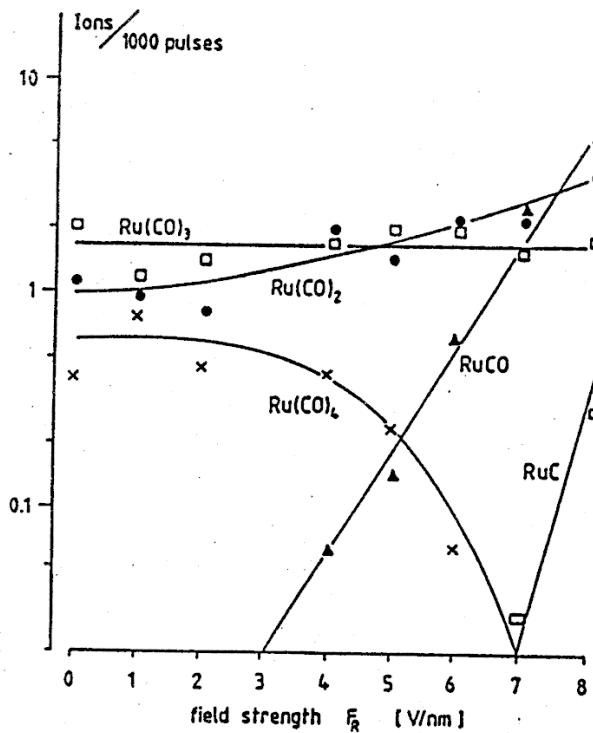


Fig. 5 Experimental intensities as function of the steady field strength, F_R . Parameters: $F_D=29$ V/nm, constant during F_R variation, $t_R=10$ ms, $T=328$ K, $p_{CO}=1.3 \cdot 10^{-4}$ Pa.

ever, is missing in the spectra. With increasing F_R the $Ru(CO)_4^{2+}$ intensity decreases and for $F_R > 7$ V/nm this species cannot be detected any longer. In contrast to this behaviour

we find increasing amounts of RuCO^{2+} , with an onset at a field strength $F_R \approx 3 \text{ V/nm}$. The $\text{Ru}(\text{CO})_2^{2+}$ ions also become slightly more abundant within the measured range of F_R values, whereas no change of the amount of $\text{Ru}(\text{CO})_3^{2+}$ is observed. It is noted that the total CO content in $\text{Ru}(\text{CO})_x^{2+}$ ($x > 2$) remains nearly constant during F_R variation.

RuCO^{2+} are considered to be formed by field desorption of CO_{ad} with simultaneous removal of the underlying lattice atom. The occurrence of the $\text{Ru}(\text{CO})_x^{2+}$ ions can be understood in terms of a consecutive surface reaction involving their neutral molecules. These species must have different dipole moments, μ , in order to observe the steady electrical field to change the relative intensities. Unfortunately, no μ values for adsorbed Ru-subcarbonyls are available. Since the influence of F_R is to increase the intensities of the low index $\text{Ru}(\text{CO})_x$ species we expect, from thermodynamic reasons, these species to have smaller dipole moments than the high index homologues.

From the reaction time variation (fig. 6) conclusions can be drawn for the kinetics of the $\text{Ru}(\text{CO})_x$ -formation.

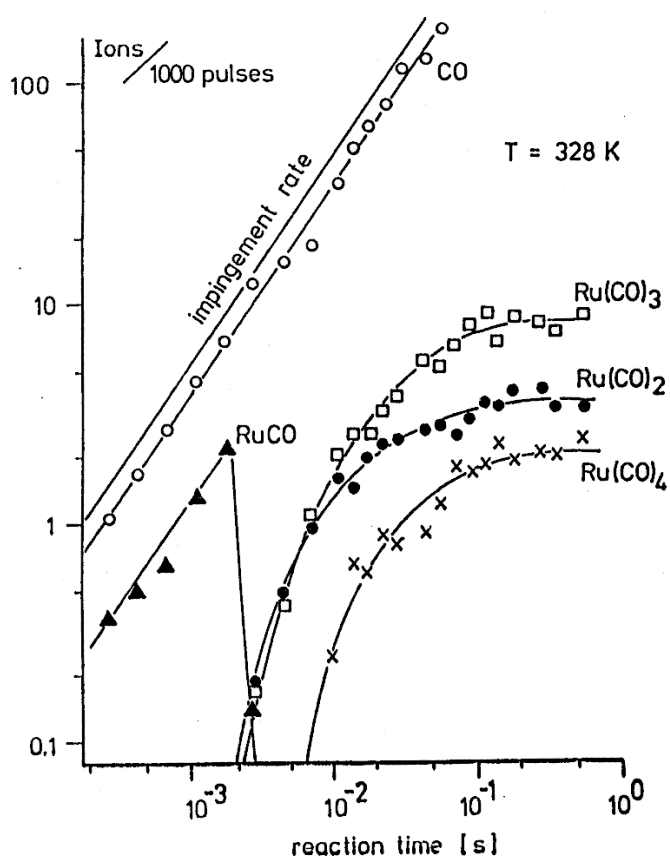


Fig. 6 Experimental intensities as function of the reaction time t_R , monitored area of about 140 surface sites (impingement rate $\approx 6.5 \text{ CO/s}$ referring to a calibrated transmission of 18 % for the mass spectrometer). Experimental parameters: $F_p = 29 \text{ V/nm}$, $F_R = 0$, $T = 328 \text{ K}$, $p_{\text{CO}} = 1.3 \cdot 10^{-4} \text{ Pa}$.

At $t_R < 2$ ms only CO^+ and RuCO^{2+} are detected. Their intensities are directly proportional to the impingement rate of CO with a sticking probability of 0.4 to 0.9, which is in agreement with other literature values [11].

At $t_R > 2$ ms Ru(CO)^{2+} disappears abruptly while Ru(CO)_2^{2+} and Ru(CO)_3^{2+} appear at nearly the same time with equal intensities. Ru(CO)_4^{2+} displays a further delay time. At long times, t_R , the intensities of the Ru(CO)_x^{2+} level off and indicate steady surface concentrations. For the Ru(CO)_3 we find higher concentrations than for the other subcarbonyl species at $T = 328$ K. The constant level portions of the concentrations indicate that the rates of formation, forward and backward reactions, counterbalance. It is observed that the Ru(CO)_2 concentration levels off first. The corresponding relaxation time, τ_R , which is the time to reach the $1-1/e$ value of the saturation concentration in a first order reaction, is $\tau_R \approx 30$ ms. This time is shorter than the respective times for Ru(CO)_3 and Ru(CO)_4 , which coincide and amount to ≈ 70 ms.

At a higher reaction temperature, $T_2 = 458$ K, the kinetic features of the Ru(CO)_x species are different, the steady Ru(CO)_3 concentration is drastically lower and only slightly above the detection limit, and Ru(CO)_4 is not seen at all. The steady Ru(CO)_2 concentration has also diminished substantially, appearing at short times t_R without any time lag. The observed temperature dependence indicates the Ru(CO)_2 formation to be associated with an activated process. It is likely that this process comprises the removal of a Ru atom from its lattice position. At $T_2 = 458$ K, CO_{ad} undergoes considerable thermal desorption from the Ru(001) terraces. Therefore, the CO_{ad} concentration is smaller than at $T_1 = 328$ K and high-index Ru(CO)_x species cannot form in significant amounts.

CONCLUSIONS

Under the influence of chemisorption layers the mobility of surface atoms is largely enhanced, as demonstrated for the metals nickel and ruthenium. The transfer of metal atoms requires that kink site lattice atoms are removed from their anchored lattice into mobile adlayer positions. This activated step can be influenced by CO-chemisorption.

Earlier investigations by FIM [12] have shown that individual nickel atoms which are evaporated onto a flat terrace of a clean (110)-Ni plane

start to move at temperatures above 140 K. Surface self-diffusion of Ni(110), investigated by macroscopic mass transfer technique [13], requires temperatures of $T > 770$ K. In our experiments temperatures of $T > 300$ K are used to remove surface lattice sites and to study surface mobility.

In the case of Ni as well as for Ru, subcarbonyls, probably with a minimum of two carbonyl groups, have to be formed in order to reduce the activation barrier for the transfer of a kink site metal atom into an ad-layer position.

In detail, the formation of subcarbonyls of nickel and ruthenium as well as the behaviour under field desorption conditions show different features which reflect differences in the kinetic behaviour of these systems.

ACKNOWLEDGEMENT

Financial support by the Deutsche Forschungsgemeinschaft Sfb 6/81 is gratefully acknowledged.

REFERENCES

1. E.W. Müller, J.A. Panitz, S.B. McLane: Rev. Sci. Instrum., 39, 83 (1968).
2. E.W. Müller, T.T. Tsong: Progr. in Surf. Sci., 4, 1 (1973).
3. G.L. Kellogg: J. Phys. E: Sci. Instrum., 20, 125 (1987).
4. J.H. Block, A.W. Czanderna, in: Methods and Phenomena, Vol. 1, p. 379, Elsevier Scientific Publ. 1975.
5. D.L. Cocke, G. Abend, J.H. Block: J. of Chem. Kinetics, 9, 157 (1977).
6. G. Abend, R.-G. Abitz, J.H. Block, in: Nonlinear Behaviour of Molecules, Atoms and Ions in Electric, Magnetic or Electromagnetic Fields, p. 261, Elsevier Scientific Publ. Comp., 1979.
7. W.A. Schmidt, J.H. Block, K.A. Becker: Surf. Sci., 122, 409 (1982).
8. D.B. Liang, G. Abend, J.H. Block, N. Kruse: Surf. Sci., 126, 392 (1983).
9. N. Kruse: Surf. Sci., 178, 820 (1986).
10. N. Kruse, G. Abend, J.H. Block, E. Gillet, M. Gillet: Journ. de Physique, C7 47, 87 (1986).
11. H. Pfnür, D. Menzel: J. Chem. Phys., 79, 2400 (1983).
12. R.T. Tung, W.R. Graham: Surf. Sci., 97, 73 (1980).
13. H.P. Bonzel, E.E. Latta: Surf. Sci., 76, 275 (1978).